

NASA/TM-2010-216692



Relating Cohesive Zone Models to Linear Elastic Fracture Mechanics

John T. Wang
Langley Research Center, Hampton, Virginia

May 2010

NASA STI Program . . . in Profile

Since its founding, NASA has been dedicated to the advancement of aeronautics and space science. The NASA scientific and technical information (STI) program plays a key part in helping NASA maintain this important role.

The NASA STI program operates under the auspices of the Agency Chief Information Officer. It collects, organizes, provides for archiving, and disseminates NASA's STI. The NASA STI program provides access to the NASA Aeronautics and Space Database and its public interface, the NASA Technical Report Server, thus providing one of the largest collections of aeronautical and space science STI in the world. Results are published in both non-NASA channels and by NASA in the NASA STI Report Series, which includes the following report types:

- **TECHNICAL PUBLICATION.** Reports of completed research or a major significant phase of research that present the results of NASA programs and include extensive data or theoretical analysis. Includes compilations of significant scientific and technical data and information deemed to be of continuing reference value. NASA counterpart of peer-reviewed formal professional papers, but having less stringent limitations on manuscript length and extent of graphic presentations.
- **TECHNICAL MEMORANDUM.** Scientific and technical findings that are preliminary or of specialized interest, e.g., quick release reports, working papers, and bibliographies that contain minimal annotation. Does not contain extensive analysis.
- **CONTRACTOR REPORT.** Scientific and technical findings by NASA-sponsored contractors and grantees.
- **CONFERENCE PUBLICATION.** Collected papers from scientific and technical conferences, symposia, seminars, or other meetings sponsored or co-sponsored by NASA.
- **SPECIAL PUBLICATION.** Scientific, technical, or historical information from NASA programs, projects, and missions, often concerned with subjects having substantial public interest.
- **TECHNICAL TRANSLATION.** English-language translations of foreign scientific and technical material pertinent to NASA's mission.

Specialized services also include creating custom thesauri, building customized databases, and organizing and publishing research results.

For more information about the NASA STI program, see the following:

- Access the NASA STI program home page at <http://www.sti.nasa.gov>
- E-mail your question via the Internet to help@sti.nasa.gov
- Fax your question to the NASA STI Help Desk at 443-757-5803
- Phone the NASA STI Help Desk at 443-757-5802
- Write to:
NASA STI Help Desk
NASA Center for AeroSpace Information
7115 Standard Drive
Hanover, MD 21076-1320

NASA/TM-2010-216692



Relating Cohesive Zone Model to Linear Elastic Fracture Mechanics

John T. Wang
Langley Research Center, Hampton, Virginia

National Aeronautics and
Space Administration

Langley Research Center
Hampton, Virginia 23681-2199

May 2010

Available from:

NASA Center for Aerospace Information
7115 Standard Drive
Hanover, MD 21076-1320
443-757-5802

RELATING COHESIVE ZONE MODELS TO LINEAR ELASTIC FRACTURE MECHANICS

John T. Wang

NASA Langley Research Center
Hampton, VA

Abstract

The conditions required for a cohesive zone model (CZM) to predict a failure load of a cracked structure similar to that obtained by a linear elastic fracture mechanics (LEFM) analysis are investigated in this paper. This study clarifies why many different phenomenological cohesive laws can produce similar fracture predictions. Analytical results for five cohesive zone models are obtained, using five different cohesive laws that have the same cohesive work rate (CWR-area under the traction-separation curve) but different maximum tractions. The effect of the maximum traction on the predicted cohesive zone length and the remote applied load at fracture is presented. Similar to the small scale yielding condition for an LEFM analysis to be valid, the cohesive zone length also needs to be much smaller than the crack length. This is a necessary condition for a CZM to obtain a fracture prediction equivalent to an LEFM result.

Introduction

The origin of the cohesive zone models (CZMs) can be traced back to the “Dugdale-Barrenblatt model” [1, 2]. The cohesive zone is considered to be a fracture processing zone ahead of the crack tip. For most cohesive laws, the traction-separation curves used to model the material within the cohesive zone are phenomenological, and hence, are not directly related to the physical process in the damage zone which typically is difficult to determine experimentally. Regardless, the CZM approach has been widely accepted as a computationally convenient fracture analysis tool. If the CZM approach is used in a finite element analysis, the crack initiation, growth, and direction of growth can be automatically determined. Many different cohesive laws with variances in maximum traction, maximum separation, and shape have been proposed; such as the linear softening cohesive law by Camacho and Ortiz [3], the exponential cohesive law by Needleman [4,5] and Xu and Needleman [6], the trapezoidal cohesive law by Tvergaard and Hutchinson [7], and the polynomial cohesive law by Tvergaard[8]. Researchers found these cohesive laws generally produce results that correlated well with experimental data such as the failure load and crack growth for cracked structures. For linear elastic materials, these predictions are comparable to linear elastic fracture mechanics (LEFM) results; however, the conditions under which the cohesive zone modeling approach and the

fracture mechanics approach are equivalent have not been systematically investigated. Here, the equivalence of the two modeling approaches means that they can predict the same failure load for a cracked structure.

The objective of this paper is to investigate under what conditions the cohesive zone model and the LEFM approach are equivalent. Linear softening cohesive laws are used in this study. The relationship between the CWR (area below the traction-separation curve of the cohesive law) and the J-integral value [9] is discussed. Integral equations, for using CZMs to analyze the fracture of an infinite plate with a crack under a remote tensile load, are presented [10]. An iterative numerical procedure is implemented as a MATLAB® M-file [11] for solving these equations to obtain the length of the cohesive zone ahead of the original crack, the opening displacements along the cohesive zone, and the remote applied stress at the moment of crack growth initiation. The effect of varying the maximum traction of a cohesive law on the predicted cohesive zone length and remote applied stress is investigated. The remote applied stress is used in an LEFM formula to determine the energy release rate. By comparing the energy release rate with the CWR, it is possible to determine whether the cohesive zone modeling approach is equivalent to the LEFM approach, i.e. whether it is able to produce a similar failure load for a cracked structure to that produced by the LEFM approach.

CWR and J-integral value

A CZM is used to study the fracture of an infinite plate with a crack length of $2a$ subjected to a remote applied tensile stress σ_∞ as shown in Figure 1a. Note that all the equations and analysis results presented in this paper are related to Mode I fracture of linear elastic material. In the cohesive zones (narrow bands) ahead of the crack tips, the prospective fracture surfaces are assumed to be restrained by a cohesive stress that Dugdale took to be the yield stress of the material [2]. The traction (cohesive stress) σ and the separation, $\delta = u_2^+ - u_2^-$, of the upper and lower prospective crack surfaces, where u_2^+ and u_2^- are the opening displacements in the y-direction for the upper and lower surfaces, respectively, are shown in Figure 1b.

A CZM model needs a cohesive law to relate the traction to the separation at the same location along the x -axis for describing the constitutive behavior of the cohesive zone. The cohesive law used in this paper is a linear softening cohesive law as shown in Figure 1c,

$$\begin{aligned} \sigma &= \sigma_c (\delta_c - \delta) / \delta_c & 0 \leq \delta \leq \delta_c \\ &= 0 & \delta > \delta_c \end{aligned} \quad (1)$$

where σ_c is the maximum traction and δ_c is the maximum separation. The cohesive work rate (CWR) Φ_c , or work of separation per unit area, is the area under the linear softening curve

$$\Phi_c = \frac{1}{2} \sigma_c \delta_c \quad (2)$$

At the moment of the crack growth initiation, the cohesive zone opening displacement at the crack tip reaches maximum separation, $\delta(a) = \delta_c$, and the cohesive zone is fully developed as shown in Figure 2 [7]. During the subsequent crack growth, the length of the cohesive zone and the opening displacement along the cohesive zone length are unchanged. The J-integral [9], taken along the boundary of a fully developed cohesive zone, the contour Γ , can be expressed as,

$$J = \int_{\Gamma} (W n_1 - T_i \frac{\partial u_i}{\partial x}) ds \quad (3)$$

where W is the strain energy per unit volume, n_1 is directional cosine between the positive side (outward) of the normal N and the x -axis, T_i is the i^{th} component of the traction perpendicular to Γ in the outward direction, u_i is the i^{th} component of the displacement, ds is an arc element of Γ .

For contour Γ shown in Figure 3, $n_1 = T_1 = 0$ and the J -integral value for a fully developed cohesive zone becomes [12]

$$\begin{aligned} J_c &= -\int_0^{\rho} \sigma \left[\frac{\partial u_2^+}{\partial x} - \frac{\partial u_2^-}{\partial x} \right] dx + J_{czt} = -\int_0^{\rho} \sigma \frac{\partial \delta}{\partial x} dx + J_{czt} \\ &= \int_0^{\delta_c} \sigma d\delta + J_{czt} = \Phi_c + J_{czt} \end{aligned} \quad (4)$$

where J_c is the critical J value immediately before the initiation of crack growth and J_{czt} is a J -integral value of an infinitesimal contour, not shown in the figure, around the cohesive zone tip. For an isotropic material, J_{czt} is related to the stress intensity factor K_{czt} , if it exists, at the cohesive zone tip

$$J_{czt} = \frac{K_{czt}^2}{E} \quad (5)$$

Since the J -integral is a path independent integral, the J value obtained from any contour integral around the cohesive zone such as Γ_1 in Figure 3 must also equal to J_c . If the cohesive zone model is equivalent to an LFM model, the stress field outside of the cohesive zone must

be near the same as the K-dominant stress field [13] in the LEFM model. In other words, the path independent J_c can be related to the fracture toughness K_c as

$$K_c = \sqrt{EJ_c} \quad (6)$$

and the critical energy release rate defined in LEFM as

$$G_c = J_c \quad (7)$$

For cohesive laws that assume the CWR to be the same as the critical energy release rate,

$$\Phi_c = G_c = J_c \quad (8)$$

the stress intensity factor at the cohesive zone tip, K_{czt} in Eq. (5), must vanish because J_{czt} must be zero to satisfy Eq. (8). Note that G_c and K_c are material properties and are experimentally determined, so Φ_c is also considered to be a material property.

Because $J_{czt} = 0$ in Eq. (4), then J_c obtained by the contour around the cohesive zone is the CWR Φ_c corresponding to the area under the traction-separation curve. Cohesive zone models with the same CWR but different shapes will produce the same J_c . If J_c is the only parameter to determine fracture, it is expected that the same failure prediction can be obtained with different shapes of the cohesive law. This may be the reason why CZMs with different shapes can generate similar failure predictions.

Analytical Solutions for Cohesive Zone Models

CZM analyses of a cracked infinite plate subjected to a remote tensile stress, as shown in Figure 1a, are presented in this section. Five linear softening cohesive laws shown in Figure 4, with different maximum tractions but all having the same CWR, were used in this study. The effects of maximum traction on the predicted cohesive zone length and remote applied stress were investigated. The predicted remote applied stresses were used in an LEFM formula to compute the energy release rate at failure. Good agreement between the energy release rate at failure and the CWR determines the equivalence of a CZM and a LEFM analysis.

The analytical procedure presented here follows the paper authored by Jin and Sun [10]. The cohesive zone is treated as an extended part of the crack with the stress intensity factor being removed at the tip of the cohesive zone. Hence,

$$\sigma_\infty \sqrt{\pi c} - \frac{2}{\sqrt{\pi c}} \int_a^c \frac{\sigma(\xi) d\xi}{\sqrt{1 - \xi^2 / c^2}} = 0 \quad (9)$$

where c is the x -coordinate of the cohesive zone tip and $\sigma(\xi)$ is the traction at location ξ as shown in Figure 1b.

The total cohesive zone opening displacement δ at location x is [14]

$$\delta(x) = \frac{4c\sigma_\infty}{E} \sqrt{1 - \frac{x^2}{c^2}} - \frac{4}{\pi E} \int_a^c G(x, \xi) \sigma(\xi) d\xi \quad (10)$$

where E is the Young's modulus, and $G(x, \xi)$ is an influence function given by

$$G(x, \xi) = \ln \left| \frac{\sqrt{1 - x^2/c^2} + \sqrt{1 - \xi^2/c^2}}{\sqrt{1 - x^2/c^2} - \sqrt{1 - \xi^2/c^2}} \right| \quad (11)$$

For the linear softening model shown in Figure 1b, Eq. (10) can be expressed as

$$\delta(x) = \frac{4c\sigma_\infty}{E} \sqrt{1 - \frac{x^2}{c^2}} - \frac{4}{\pi E} \int_a^c G(x, \xi) \frac{\sigma_c(\delta_c - \delta(\xi))}{\delta_c} d\xi \quad (12)$$

and Eq. (9) can be expressed as

$$\sigma_\infty = \frac{2\sigma_c}{\pi c} \left(-\int_a^c \frac{\delta(\xi)/\delta_c}{\sqrt{1 - \xi^2/c^2}} d\xi + \int_a^c \frac{d\xi}{\sqrt{1 - \xi^2/c^2}} \right) \quad (13)$$

Substituting σ_∞ into Eq. (12), an integral equation is obtained for determining the cohesive zone length, $\rho = c - a$, and cohesive zone opening displacements (CZODs) $\delta(x)$

$$\begin{aligned} & \frac{\pi E \delta^*(x) \Phi_c}{2c\sigma_c^2} - \frac{1}{c} \int_a^c G(x, \xi) \delta^*(\xi) d\xi + \frac{2}{c} \sqrt{1 - \frac{x^2}{c^2}} \int_a^c \frac{\delta^*(\xi)}{\sqrt{1 - \xi^2/c^2}} d\xi \\ & = \frac{2}{c} \sqrt{1 - \frac{x^2}{c^2}} \int_a^c \frac{d\xi}{\sqrt{1 - \xi^2/c^2}} - \frac{1}{c} \int_a^c G(x, \xi) d\xi \end{aligned} \quad (14)$$

where $\delta^*(x) = \delta(x) / \delta_c$.

Equation 14 can be solved with an iterative method shown in Figure 5, in which an initial cohesive zone length $\rho = c - a$ is given first to determine the integral interval, $[a, c]$, for the

integral terms in Eq. (14) and then the CZODs along $c-a$ are computed. If the predicted opening displacement at the crack tip $\delta(a)$ is not equal to the maximum separation δ_c , an updated cohesive length is given until the $\delta(a)$ equals δ_c . The final value of $c-a$ is the cohesive zone length ρ . The remote applied stress σ_∞ can be obtained with Eq. (13), by using the final set of CZODs. The remote applied stress is used to compute the energy release rate using the following LEFM formulae,

$$G(\sigma_\infty) = \frac{\pi a \sigma_\infty^2}{E} \quad (15)$$

If the ratio of the computed energy release rate $G(\sigma_\infty)$ to the CWR, Φ_c , is close to unity, then the CZM is considered to be equivalent to an LEFM analysis.

Results

Analytical results for five cohesive law models with different maximum tractions as shown in Figure 4 are presented in this section. All the results are computed at the initiation of crack growth when the cohesive zone is fully developed. The effect of maximum tractions on cohesive zone length, remote applied stress, the equivalence of CZM approach and LEFM analysis is presented. The effect of maximum traction on cohesive zone length can be found in Figure 6, which shows that larger maximum tractions result in shorter cohesive zone lengths, ρ . Two curves represent results obtained with two different crack lengths, one has $a/l_{ch} = 1$ and the other one has $a/l_{ch} = 10$. Note that l_{ch} is a characteristic length, and in this paper it is defined based on Model B in Figure 4,

$$l_{ch} = \frac{E\Phi_c}{\sigma_c^2} \quad (16)$$

For the rest of the paper, the term crack length means the half-crack length a in Figure 1a. The two curves in Figure 6 are converged for maximum tractions greater than $2\sigma_c$, indicating that the cohesive zone length may not depend on the crack length for a cohesive law with a large maximum traction. However, the cohesive zone lengths depend on crack length for models with a maximum traction less than σ_c . The cohesive zone length for the short crack $a/l_{ch} = 1$ is longer than that of the long crack $a/l_{ch} = 10$.

Cohesive zone lengths are predicted for all five cohesive law models in Figure 4. The cohesive zone length reaches a constant value for all cohesive law models as the crack length increases. For illustration purposes, only results of Models A, B, and D are plotted in Figure 7. Models A, B, and D have maximum tractions of $1/2\sigma_c$, σ_c , and $2\sigma_c$, respectively. For the largest

maximum traction $2\sigma_c$ model, the cohesive zone length reaches a constant value at a crack length around $a = 2l_{ch}$. For the second largest maximum traction σ_c model, the cohesive zone length reaches a constant value at a crack length around $a = 5l_{ch}$. The cohesive zone length almost reaches a constant value at $a = 16l_{ch}$ for the model with the smallest maximum traction of $1/2 \sigma_c$.

The cohesive zone opening displacements along the cohesive zone length for models with different maximum tractions are plotted in Figure 8. There are three cohesive zone opening displacement curves associated with three cohesive laws with maximum tractions of $1/2\sigma_c$, σ_c , and $2\sigma_c$, respectively. These cohesive zone opening displacement curves along the cohesive zone length are not linear (the shape of the cohesive zone is a cusp). Figure 8 also shows that the smaller the maximum traction results in the longer the cohesive zone length. These opening displacements are used in Eq. (13) to compute the remote applied stresses.

The computed remote stresses as a function of the maximum traction of all five CZM models are plotted in Figure 9. There are two curves shown on Figure 9 representing two different crack lengths. The bottom curve shows that the remote applied stresses for the longer crack length of $a = 10l_{ch}$ reaches a constant value for maximum traction greater than one σ_c , but the top curve for the shorter crack length of $a = l_{ch}$ shows that the remote applied stresses has not reached a constant value for the maximum traction at $4 \sigma_c$.

The computed remote applied stresses are then used in Eq. (15) to compute LEFM energy release rates $G(\sigma_\infty)$. The ratio of $G(\sigma_\infty)$ to Φ_c is defined as the normalized LEFM energy release rate (NLERR). If the NLERR is near unity, then the cohesive zone model is equivalent to an LEFM analysis, and both models would predict the same failure load. The NLERR as a function of maximum traction is plotted in Figure 10. The figure shows that for a long crack length, $a = 10l_{ch}$, the NLERR approaches unity for maximum tractions greater than $2\sigma_c$ while for a short crack length, $a = l_{ch}$, the NLERR reaches unity at a much slower rate (a cohesive law with a maximum traction greater than $4\sigma_c$ needs be used).

The NLERR requires high tractions to reach unity for the shorter crack length $a = l_{ch}$ because the cohesive zone length relative to the crack length is not small ($\ll 1$). This large cohesive zone length, similar to a large scale yielding zone, may significantly alter the original K dominant stress field around the crack tip [13]. Hence, the results from the CZM model cannot be equivalent to an LEFM analysis. To confirm this hypothesis, the NLERR as a function of the ratio of cohesive zone length to crack length is plotted in Figure 11 for both the crack lengths. This plot reveals that the two curves shown in Figure 10 can be collapsed to become a single

curve. This indicates that the ratio of cohesive zone length to the crack length may be an important parameter for fracture predictions using CZM. The ratio of cohesive zone length to crack length, ρ/a , must be close to zero for the CZM to be equivalent to an LEFM analysis. Physically, this means that regions ahead of the crack tip that exhibit mechanisms other than brittle fracture (plasticity, bridging fibers, etc) must be very small relative to the crack length for LEFM to be valid, and hence, for the CZM approach to be equivalent to LEFM.

Summary

A MATLAB® M-file was implemented for numerically solving the CZM integral equations with an iterative procedure. Linear softening cohesive laws with a constant CWR but different maximum tractions were used for modeling the traction-separation behavior in the cohesive zone. Results show that a reduced cohesive zone length is predicted for a cohesive model with a large maximum traction, and the ratio of cohesive zone length to the crack size needs be very small for the prediction from the CZM to be equivalent to an LEFM analysis.

The conditions required for a cohesive zone model and an LEFM analysis to be equivalent were identified from this study and other published literature. These conditions are as follows:

1. Stress intensity factor at a fully developed cohesive zone tip needs to vanish if the J-integral value around the cohesive zone is set equal to the cohesive work rate.
2. If the J-integral value around a fully developed cohesive zone is the only parameter to determine failure, then the maximum traction of a cohesive law can be changed while keeping the CWR constant without affecting the failure load prediction.
3. The ratio of the cohesive zone length to the crack length needs to be small, so the existence of the cohesive zone cannot significantly change the stress field near the crack tip.
4. The maximum traction of a CZM needs to be high. High maximum tractions result in a short cohesive zone length.

Acknowledgement

The author would like to acknowledge the helpful discussions with Professors C. T. Sun of Purdue University and Z. H. Jin of The University of Maine, and the in-depth review by his colleague Dr. T. K. O'Brien.

References

1. Barenblatt, G. I., "The mathematical theory of equilibrium cracks in brittle fracture," *Advances in Applied Mechanics*, Vol. 7. Academic Press, New York, 1962, pp. 55–129.

2. Dugdale, D. S., "Yielding of steel sheets containing slits," *Journal of the Mechanics and Physics of Solids*, Vol. 8, 1960, pp. 100–104.
3. Camacho, G. T., Ortiz, M., "Computational modelling of impact damage in brittle materials," *International Journal of Solids and Structures*, Vol. 33, 1996, pp. 2899–2938.
4. Needleman, A., "A continuum model for void nucleation by inclusion debonding," *ASME Journal of Applied Mechanics*, Vol. 54, 1987, pp. 525–531.
5. Needleman, A., "An analysis of decohesion along an imperfect interface," *International Journal of Fracture*, Vol. 42, 1990, pp. 21–40.
6. Xu X. P., Needleman A., "Void nucleation by inclusions debonding in a crystal matrix," *Modelling and Simulation in Materials Science and Engineering*, Vol. 1, 1993, pp. 111–132.
7. Tvergaard V., Hutchinson J. W., "The relation between crack growth resistance and fracture process parameters in elastic–plastic solids," *Journal of the Mechanics and Physics of Solids*, Vol. 40, 1992, pp. 1377–1397.
8. Tvergaard V., "Effect of fibre debonding in a whisker-reinforced metal," *Materials Science and Engineering A*, Vol. 125, 1990 pp. 203–213.
9. Rice, J. R., "A path independent integral and approximate analysis of strain concentration by notches and cracks," *ASME Journal of Applied Mechanics*, Vol. 35, 1968, pp. 379–386.
10. Jin, Z. H., Sun, C. T., "Cohesive fracture model based on necking," *International Journal of Fracture*, Vol. 134, 2005, pp. 91-108.
11. MATLAB® (a high-performance technical computing environment), product of The MathWorks Inc., <http://www.mathworks.com>.
12. Kanninen, M. F. and Popelar, C. H., *Advanced Fracture Mechanics*, Oxford University Press, New York, 1985.
13. Broek, D., *Elementary Engineering Fracture Mechanics*, 4th revised edition, Martinus Nijhoff Publishers, Dordrecht, 1986.
14. Tada, H., Paris, P. C. and Irwin, G. R., *The Stress Analysis of Cracks Handbook*. ASME Press, New York, 2000.

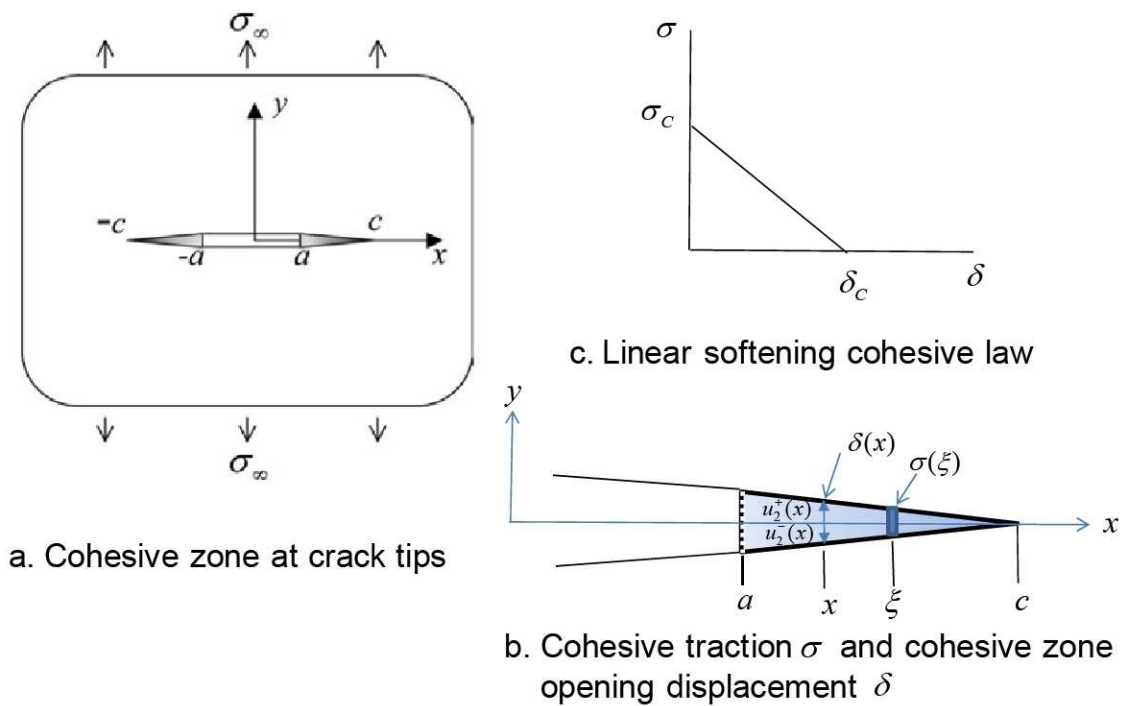


Figure 1 Fracture analysis of a cracked infinite plate using a cohesive zone model.

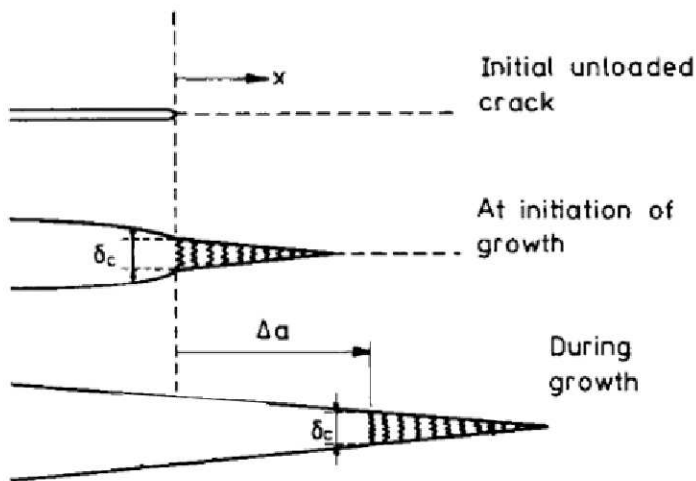


Figure 2 Cohesive zone fully developed at crack growth initiation and unchanged during growth [7].

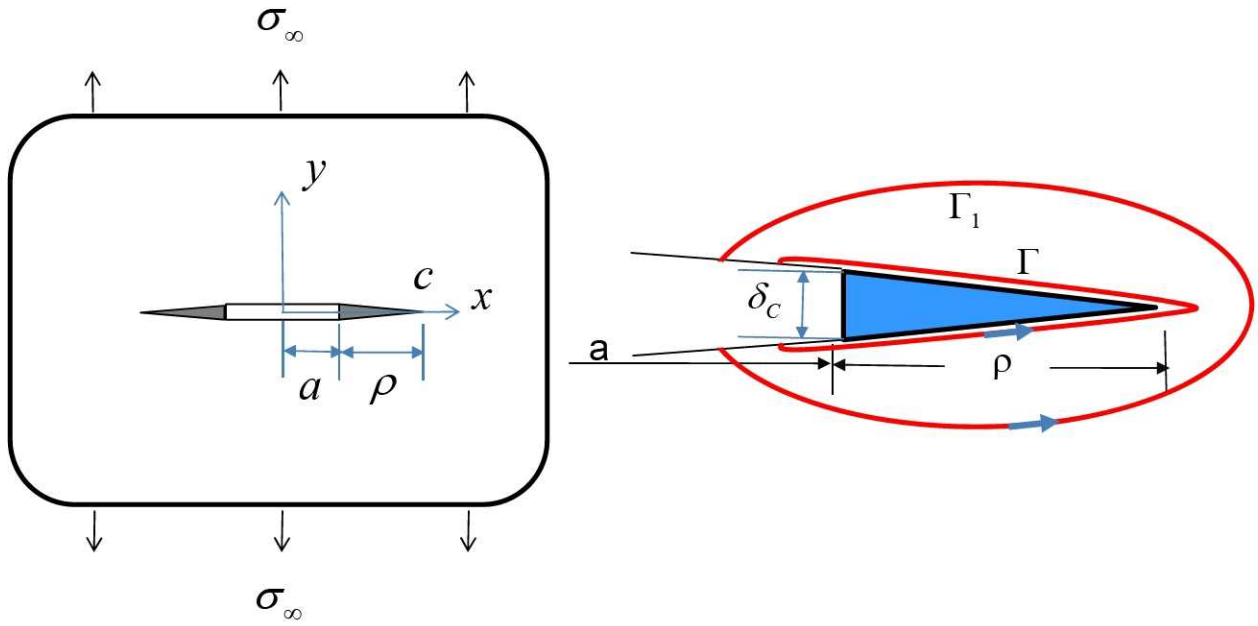


Figure 3 J-integral paths around the cohesive zone.

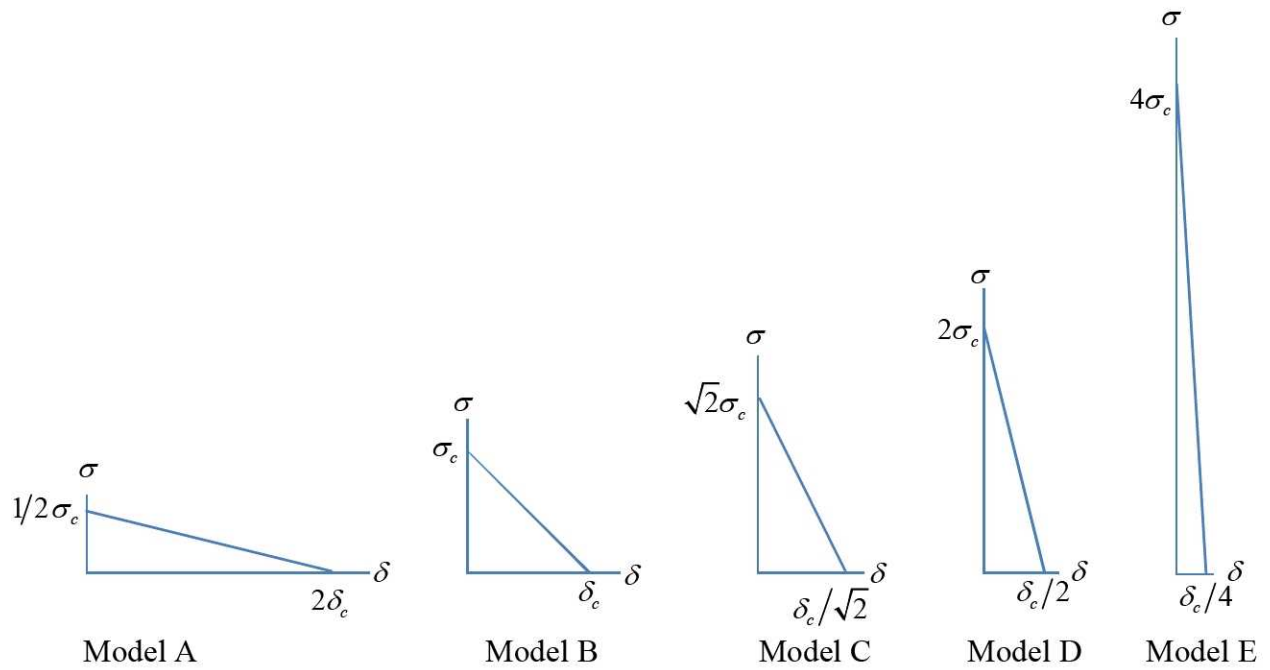


Figure 4 Five cohesive laws with the same cohesive work rate.

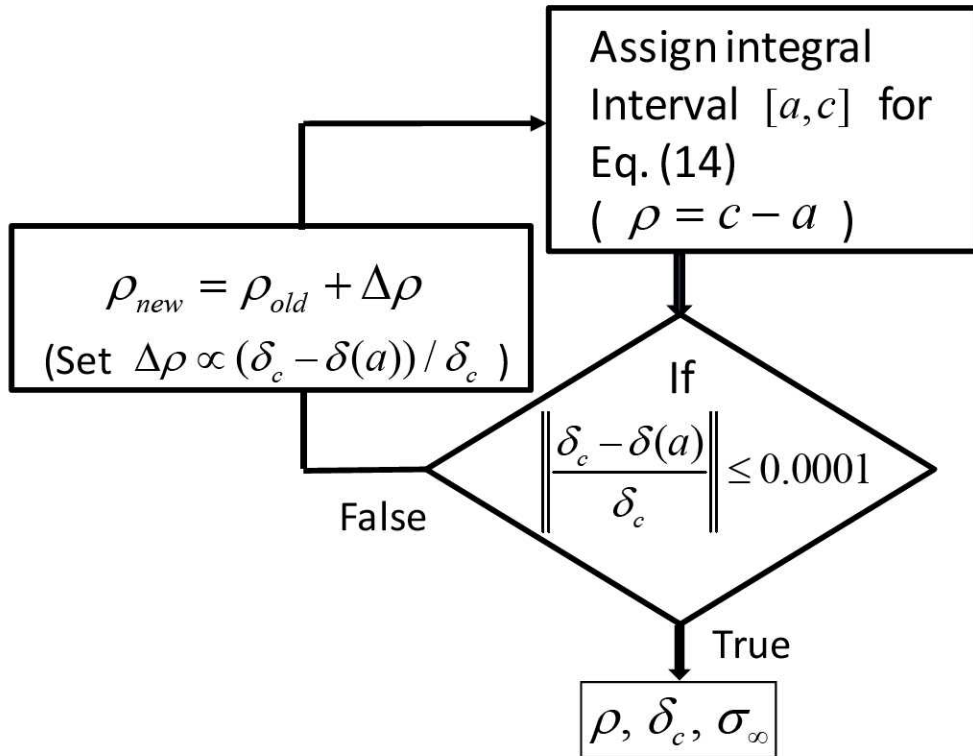


Figure 5 Solution procedure of the iterative method.

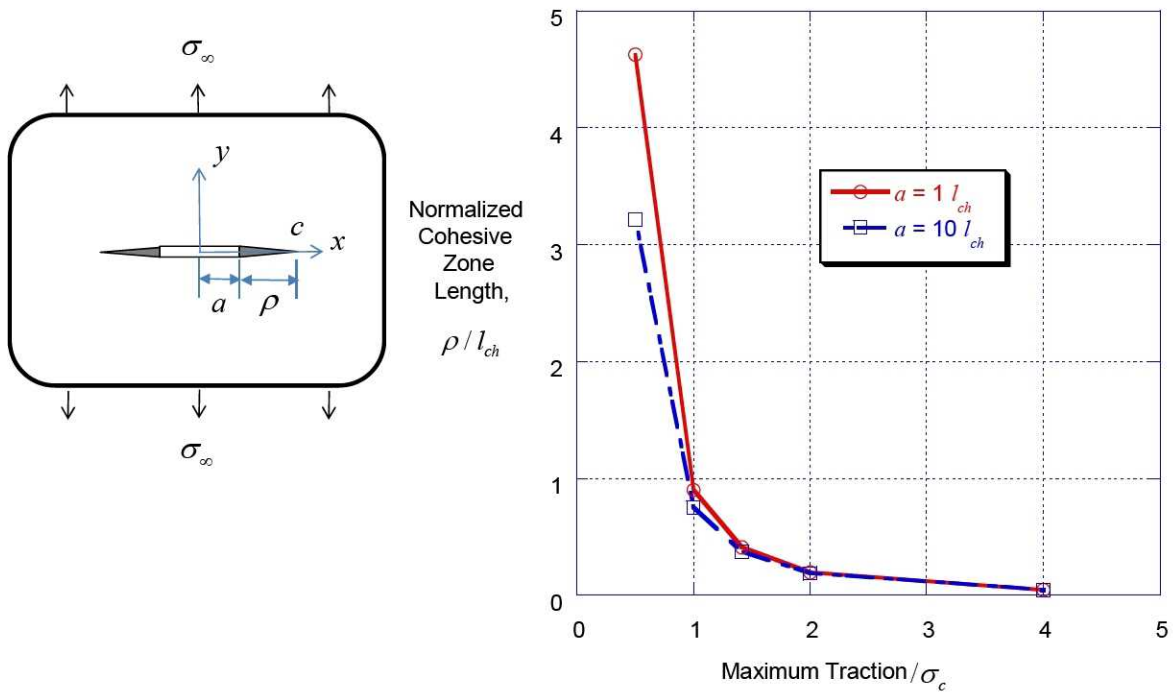


Figure 6 Cohesive zone lengths as a function of maximum traction of different cohesive laws.

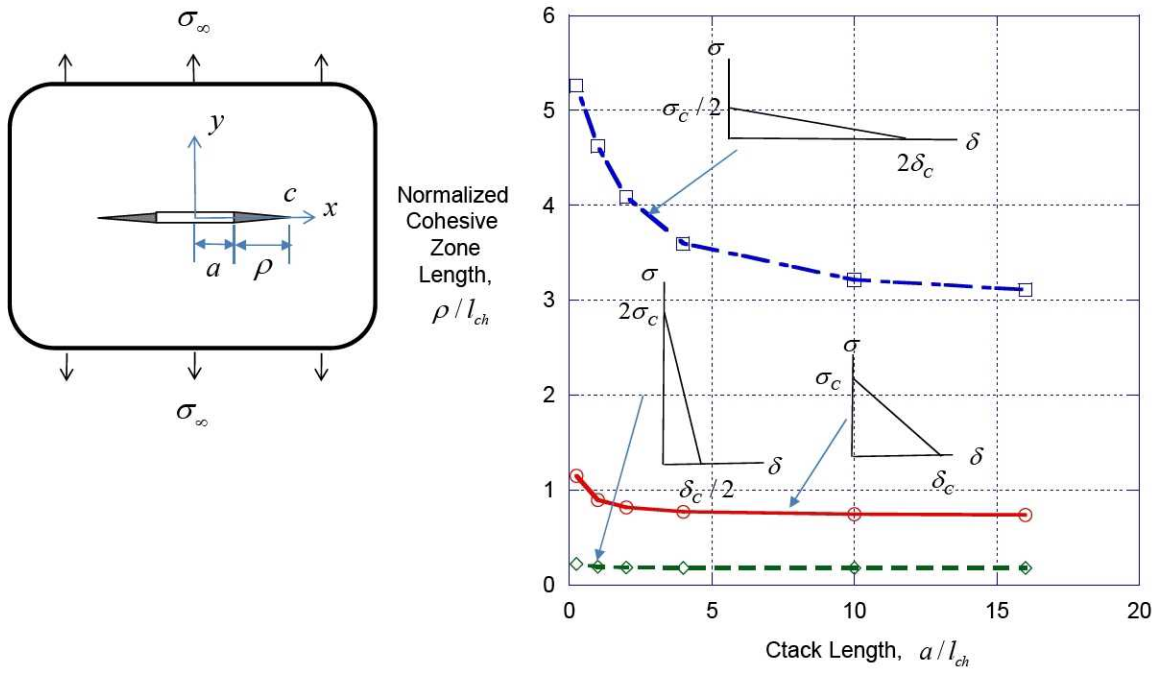


Figure 7 Cohesive zone lengths vs. crack length for models with different maximum tractions.

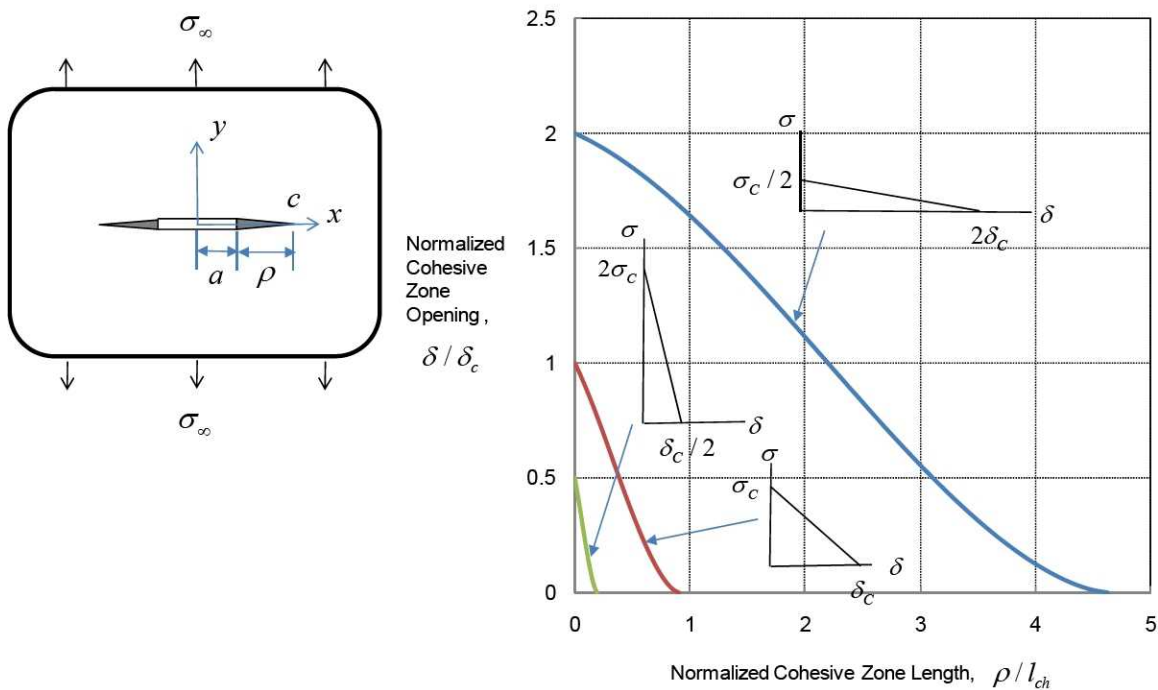


Figure 8 Cohesive opening displacements along the cohesive zone length for models with different maximum tractions ($a = 1l_{ch}$).

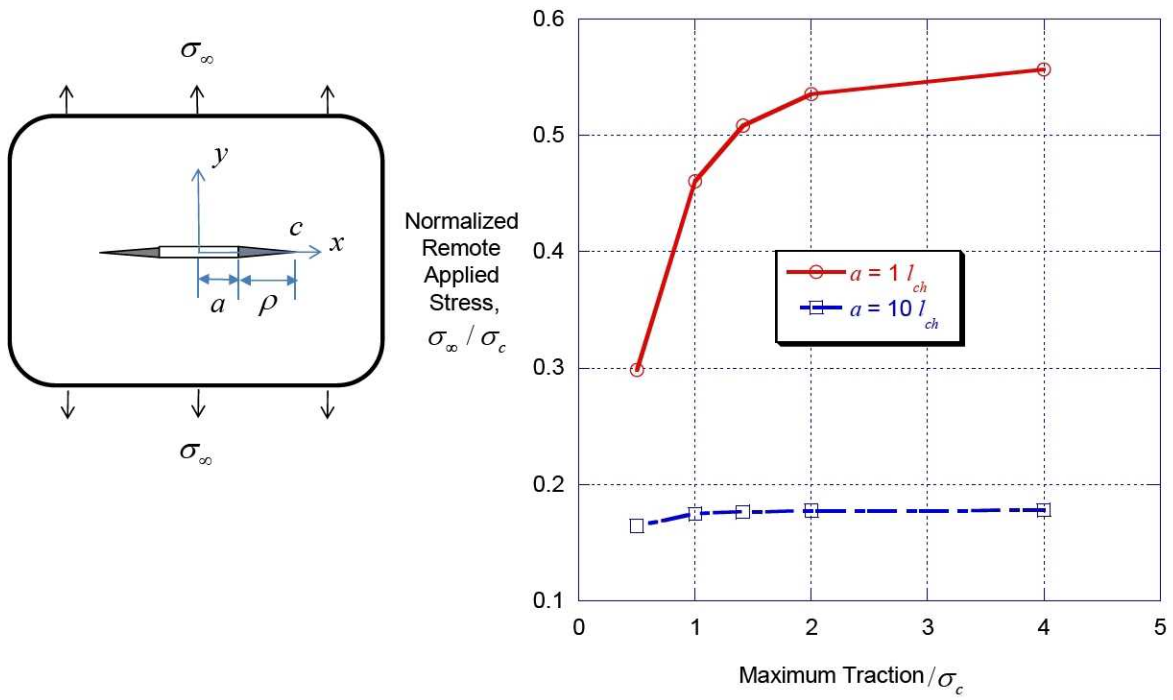


Figure 9 Remote applied stress for models with different maximum tractions.

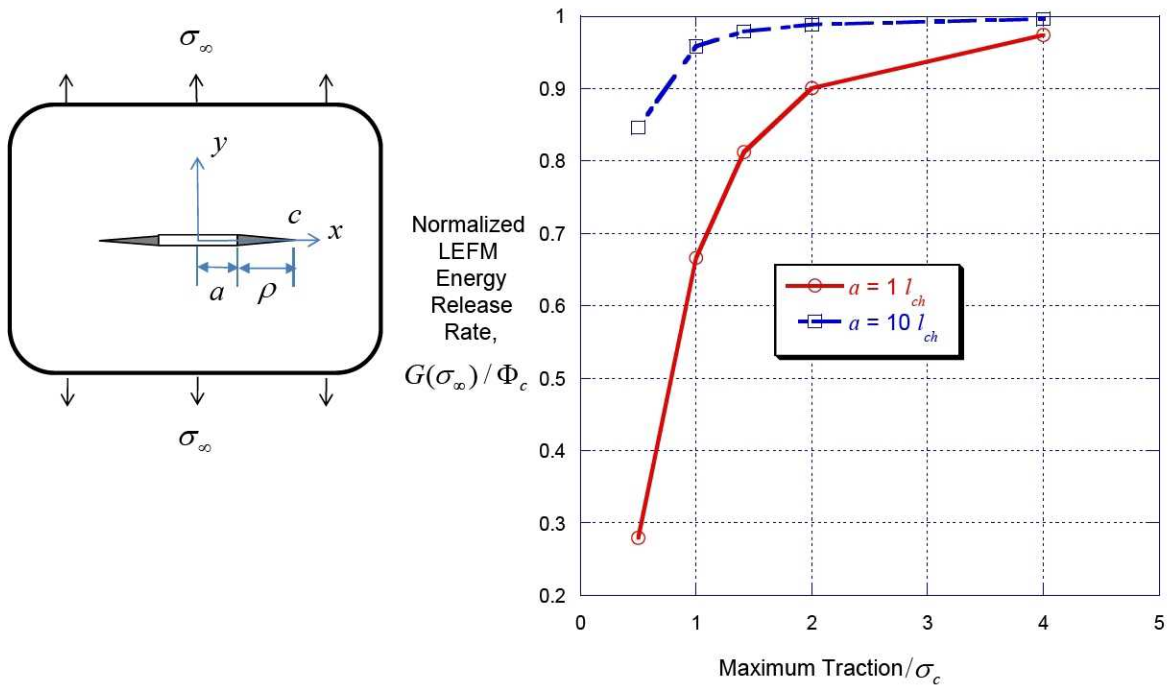


Figure 10 LEFM energy release rates for cohesive laws with different maximum tractions.

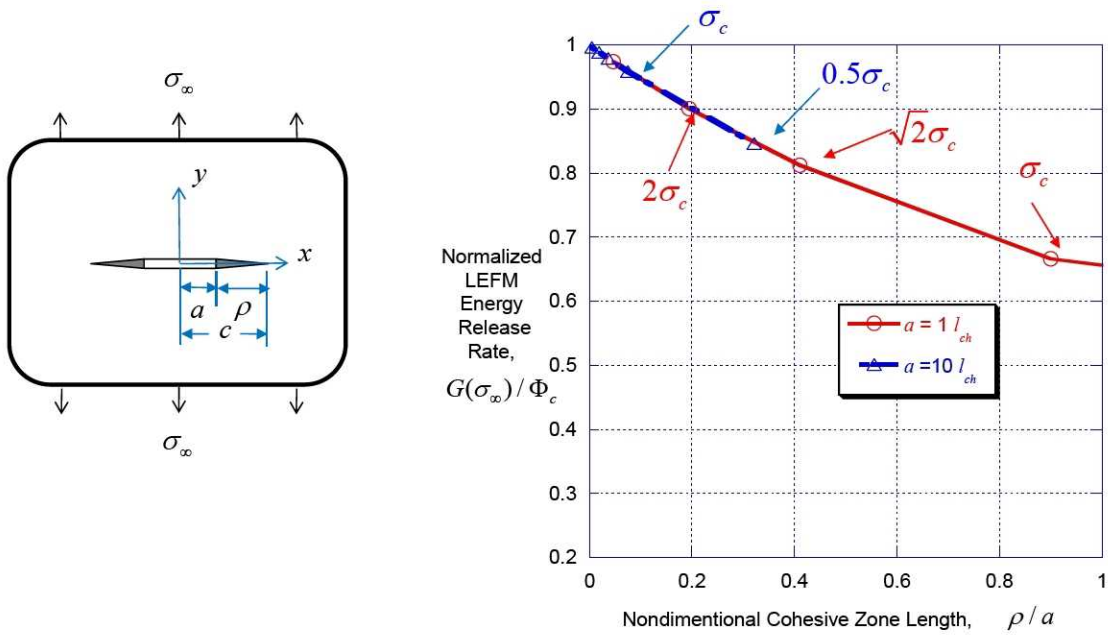


Figure 11 LEFM energy release rates at the moment of growth initiation as a function of the ratio of cohesive zone length to crack length.

REPORT DOCUMENTATION PAGE

*Form Approved
OMB No. 0704-0188*

The public reporting burden for this collection of information is estimated to average 1 hour per response, including the time for reviewing instructions, searching existing data sources, gathering and maintaining the data needed, and completing and reviewing the collection of information. Send comments regarding this burden estimate or any other aspect of this collection of information, including suggestions for reducing this burden, to Department of Defense, Washington Headquarters Services, Directorate for Information Operations and Reports (0704-0188), 1215 Jefferson Davis Highway, Suite 1204, Arlington, VA 22202-4302. Respondents should be aware that notwithstanding any other provision of law, no person shall be subject to any penalty for failing to comply with a collection of information if it does not display a currently valid OMB control number.
PLEASE DO NOT RETURN YOUR FORM TO THE ABOVE ADDRESS.

1. REPORT DATE (DD-MM-YYYY) 01-05-2010		2. REPORT TYPE Technical Memorandum		3. DATES COVERED (From - To)	
4. TITLE AND SUBTITLE Relating Cohesive Zone Model to Linear Elastic Fracture Mechanics				5a. CONTRACT NUMBER	
				5b. GRANT NUMBER	
				5c. PROGRAM ELEMENT NUMBER	
6. AUTHOR(S) Wang, John T.				5d. PROJECT NUMBER	
				5e. TASK NUMBER	
				5f. WORK UNIT NUMBER 698259.02.07.07.03.03	
7. PERFORMING ORGANIZATION NAME(S) AND ADDRESS(ES) NASA Langley Research Center Hampton, VA 23681-2199				8. PERFORMING ORGANIZATION REPORT NUMBER L-19873	
9. SPONSORING/MONITORING AGENCY NAME(S) AND ADDRESS(ES) National Aeronautics and Space Administration Washington, DC 20546-0001				10. SPONSOR/MONITOR'S ACRONYM(S) NASA	
				11. SPONSOR/MONITOR'S REPORT NUMBER(S) NASA/TM-2010-216692	
12. DISTRIBUTION/AVAILABILITY STATEMENT Unclassified - Unlimited Subject Category 39 Availability: NASA CASI (443) 757-5802					
13. SUPPLEMENTARY NOTES					
14. ABSTRACT The conditions required for a cohesive zone model (CZM) to predict a failure load of a cracked structure similar to that obtained by a linear elastic fracture mechanics (LEFM) analysis are investigated in this paper. This study clarifies why many different phenomenological cohesive laws can produce similar fracture predictions. Analytical results for five cohesive zone models are obtained, using five different cohesive laws that have the same cohesive work rate (CWR-area under the traction-separation curve) but different maximum tractions. The effect of the maximum traction on the predicted cohesive zone length and the remote applied load at fracture is presented. Similar to the small scale yielding condition for an LEFM analysis to be valid, the cohesive zone length also needs to be much smaller than the crack length. This is a necessary condition for a CZM to obtain a fracture prediction equivalent to an LEFM result.					
15. SUBJECT TERMS Cohesive zone model, Linear elastic fracture mechanics, Cohesive work rate, Energy release rate					
16. SECURITY CLASSIFICATION OF:			17. LIMITATION OF ABSTRACT	18. NUMBER OF PAGES	19a. NAME OF RESPONSIBLE PERSON
a. REPORT	b. ABSTRACT	c. THIS PAGE			STI Help Desk (email: help@sti.nasa.gov)
U	U	U	UU	20	19b. TELEPHONE NUMBER (Include area code) (443) 757-5802